Atmospheric Research 260 (2021) 105697

Contents lists available at ScienceDirect

Atmospheric Research

journal homepage: www.elsevier.com/locate/atmosres

Analysis of the October 2014 subtropical cyclone using the WRF and the HARMONIE-AROME numerical models: Assessment against observations

L. Quitián-Hernández [a,b], P. Bolgiani [a], D. Santos-Muñoz [c], M. Sastre [a,b,*], J. Díaz-Fernández [a], J. J. González-Alemán [a], J.I. Farrán [b], L. Lopez [d], F. Valero [a,e], M.L. Martín [b,e]

[a] Department of Earth Physics and Astrophysics, School of Physics, Complutense University of Madrid, Ciudad Universitaria s/n, 28040 Madrid, Spain
[b] Department of Applied Mathematics, School of Computer Engineering, University of Valladolid, Pza. de la Universidad, 1, 40005 Segovia, Spain
[c] High Resolution Limited Area Model Consortium (HIRLAM), Spain
[d] Atmospheric Physics Group, IMA, University of León, León, Spain
[e] Interdisciplinary Mathematical Institute (IMI), Complutense University of Madrid, Ciudad Universitaria s/n, 28040 Madrid, Spain

ARTICLE INFO

Keywords:
WRF model
HARMONIE-AROME model
Numerical modeling
Subtropical cyclones
MSG-SEVIRI satellite products

ABSTRACT

Subtropical cyclones (STCs) are low-pressure systems characterized by having a thermal hybrid structure and sharing tropical and extratropical characteristics. These cyclones are widely studied due to their harmful impacts, in some cases, similar to those caused by hurricanes or tropical storms. From a numerical modeling point of view, they are considered a challenge on account of their rapid intensification. That is the reason why this paper analyzes the simulations of the STC that occurred in October 2014 near the Canary Islands through two high-resolution numerical models: Weather Research and Forecasting (WRF) and HARMONIE-AROME. In this study, the simulations obtained with both models of this STC are analyzed versus different observational data. METAR data are used to validate some surface simulated variables throughout the STC life while soundings are chosen to study the tropospheric behavior. Finally, MSG-SEVIRI satellite brightness temperature is used to be compared to those brightness temperatures simulated by both models to give information of the cloud top spatial structure of this atmospheric system. The 2 m temperature, 2 m dew-point temperature, and 10 m wind speed variables do not show significant deviations when carrying out the validation of both models against the available METAR data. It is outstanding the good results found for the HARMONIE-AROME model when analyzing the temperature sounding for both analyzed dates. Additionally, regarding the wind speed sounding, better results are presented in general by the HARMONIE-AROME model, being the WRF model slightly better during the pre-STC stage. Moreover, the skillfulness of the HARMONIE-AROME model is highlighted when simulating the infrared brightness temperature and cloud distribution compared to the WRF model.

1. Introduction

The genesis and intensification of subtropical cyclones (STCs) are acquiring more importance over the years since they are sometimes part of the subtropical transitions experienced by more damaging phenomena, such as tropical cyclones or hurricanes (Steward, 2001; Davis and Bosart, 2004; Guishard et al., 2007; Dias Pinto et al., 2013; González-Alemán et al., 2015). STCs are hybrid thermal meteorological structures that share both, tropical and extratropical characteristics (Evans and Guishard, 2009). Therefore, their impact substantially resembles those caused by tropical cyclones or hurricanes (Evans and Guishard, 2009). Moreover, there is a powerful connection of the STCs strength to the atmospheric dynamics and to, among others, the diabatic processes that develop over the ocean and the sea surface temperature (Evans and Guishard, 2009; González-Alemán et al., 2015). Therefore, due to climate change, the growing concern regarding the deviation to the north of their typical trajectories leads the scientific and forecasting community to carry out a more exhaustive analysis of these events (González-Alemán et al., 2018).

Quitián-Hernández et al. (2016) performed a synoptic and mesoscale study to characterize a cyclone that occurred in October 2014 near the Canary Islands as an STC category event by analyzing its dynamical and thermal evolution. This system caused substantial economic and social damages like floodings, landslides, injured people due to a fire produced

* Corresponding author at: Department of Earth Physics and Astrophysics, School of Physics, Complutense University of Madrid, 28040 Madrid, Spain.
E-mail address: msastrem@ucm.es (M. Sastre).

https://doi.org/10.1016/j.atmosres.2021.105697
Received 15 February 2021; Received in revised form 18 May 2021; Accepted 23 May 2021
Available online 26 May 2021

by electrical storms and, unfortunately, a deceased person. The same STC was taken as a reference by Quitián-Hernández et al. (2018) to study the genesis and numerical modeling of this type of cyclones, by examining different parameterizations of the Weather Research and Forecasting (WRF) model (Skamarock and Klemp, 2008). In their study, the cumulus Tiedtke scheme (Tiedtke, 1989) was revealed as the optimum parameterization for simulating the deep convection and characterizing the cyclone as STC via the Cyclone Phase Space (CPS) diagrams (Hart, 2003). Finally, a third study of the October 2014 event was carried out by the authors focusing on the role played by the surface turbulent heat fluxes from the ocean during the genesis and intensification (Quitián-Hernández et al., 2020) of the STC. This latter study remarked the crucial role played by these heat fluxes for the intensification of the event as well as the developed Shapiro-Keyser-like STC or, in other words, bent-back warm/occluded front that underwent a warm seclusion process (Bentley and Metz, 2016).

In the present paper, the October 2014 STC is once more evaluated, although using the numerical weather prediction (NWP) HARMONIE-AROME model as a research tool. This model has been developed through the collaboration of the 10 European National Meteorological Services (NMSs), which are part of the international research High-Resolution Limited Area Model (HIRLAM) program, together with the 16 countries that comprise the Aire Limitée Adaptation Dynamique Développement International (ALADIN) project. The HARMONIE-AROME (hereafter HARMONIE) has usually been used as an operational model and as a consequence, its use and validation results are not in the public domain. However, in October 2020 the European Centre for Medium-Range Weather Forecasts (ECMWF) announced that it was moving towards an open data policy, which marks a before and after in the innovation regarding further scientific research as well as the development and improvement of weather applications. It also sets a trend in the weather research community. Thus, the HIRLAM consortium is to follow suit, and the HARMONIE model is beginning to be used for academic and research purposes (Neyestani et al., 2018; Toros et al., 2018; Fernández-González et al., 2019; Román-Cascón et al., 2019). However, to the authors' knowledge, this is the first time this model is used to simulate an STC, which creates new opportunities but also yields several challenges. Due to this novelty, the existing academic experience and research knowledge of the model is very rare and, accordingly, the literature turns out to be very sparse. This represents a challenge for the discussion of the results.

The HIRLAM consortium, initiated in 1985, was the first one developed on limited area modeling in Europe. Its prime goal is to provide operational weather forecasts for the different members of the consortium with special attention to the detection and prediction of extreme weather and its relation to public safety. The consortium validates the HARMONIE model results using an integrated verification package able to assess a statistical analysis of the model outputs including the calculation of certain statistical scores, histograms, and scattergrams, as well as other significant magnitudes (Yang, 2008). Moreover, this package is developed with data quality control and among the verification parameters, it includes the temperature and dew-point temperature, relative humidity, wind speed, or cloud cover. Furthermore, the wide expertise on numerical modeling of each of the European meteorological services that make up the HIRLAM consortium ensures the quality of the model and its outcomes. In consequence, and considering the scarcity of literature, the HIRLAM verification is taken as a reference for validating the results of this work.

In order to assess the HARMONIE performance in simulating events such as STCs, simulations of the above-mentioned October 2014 system are carried out and compared to those made using the WRF model. To do this, observational data from six different airports in the vicinity of the cyclone is assessed for surface validation throughout the cyclone life. Then, a vertical analysis of the atmosphere during the genesis and intensification of the cyclone is carried out throughout the evaluation of a sounding. According to the methodology used by Quitián-Hernández et al. (2018, 2020), this analysis is focused on two specific dates, the pre-STC stage (19 October 2014 at 1800 UTC), when the cyclone has a purely extratropical nature, and the pure-STC stage (20 October 2014 at 1800 UTC), when the cyclone has acquired subtropical characteristics. In this way, the differences between both crucial stages can be evaluated better. Moreover, an analysis through several skill scores applied to the brightness temperature (BT) field gives an observational added weight to the testing of both models in the analyzed dates. For these BT results, simulated pseudo-satellite images of both models are compared to the Meteosat Second Generation (MSG) Spinning Enhanced Visible and InfraRed Imager (SEVIRI) satellite products. Due to the difficulty of acquiring observational data in the surroundings of a damaging phenomenon of this type (scarce observation platforms and malfunctions of those produced by the cyclone), the use of satellites for the analysis is becoming an essential tool over the last years. Satellite imagery allows to evaluate the cloud top structure, which is an interesting characteristic of cyclones. In particular, there are some infrared (IR) channels that are known to be the best in terms of detecting the cloud distribution because they are in an area of the spectrum where the atmosphere is transparent to radiation, named as IR atmospheric window.

This paper is organized as follows: datasets and methodology are presented in Section 2. Section 3 includes the results and discussion for the surface validation (Section 3.1), vertical validation by means of sounding evaluation (Section 3.2), and spatial distribution (Section 3.3) via the analysis of the BT and cloud distribution. Finally, the major conclusions are summarized in Section 4.

2. Data and methodology

2.1. Numerical weather prediction models

In this study, several simulations of the October 2014 event by two high-resolution mesoscale NWP models are going to be assessed. On the one hand, the already settled and highly approved non-hydrostatic Advanced WRF model version 4.0.3 (Skamarock and Klemp, 2008) and on the other hand, the non-hydrostatic semi-Lagrangian and semi-Implicit HARMONIE model (Bengtsson et al., 2017).

The WRF numerical model is configured with a single domain of 2.5 km of grid resolution (Fig. 1), using 813 grid points in the west-east direction, 647 grid points in the south-north direction and 65 sigma levels unequally spaced, with a greater amount of levels in the lower troposphere for a better representation of the convective planetary boundary-layer processes. Adaptative time steps are used. The WRF physics options used in this study are those defined as the default for Hurricane research mode (see the Hurricane application options on the WRF User Guide 4.0, http://www2.mmm.ucar.edu/wrf/users/docs/user_guide_V4/WRFUsersGuide.pdf). Among them, it is worth noting the WRF Single-Moment 6-class (WSM6) (Hong and Lim, 2006) parameterization scheme for microphysics, YSU for the planetary boundary layer (PBL), and Dudhia (Dudhia, 1989) and RRTM for short and longwave radiation, respectively. No cumulus parameterization scheme is used in this study, being cloudiness explicitly computed by the model. In regards to this decision, it needs to be remarked that the use of convective parameterization (CP) schemes when simulating deep convective systems over high-resolution grids still remains controversial (Sun et al., 2013; Sun et al., 2014). These resolutions, which approximately range from 1 km to 10 km, are named as "grey-zone resolution" by Gerard (2007). While several studies (Kotroni and Lagouvardos, 2004; Deng and Stauffer, 2006) support the idea of using CP for those resolutions when simulating convective processes, others like Liu et al. (1997) think it is not necessary and, therefore, the model would explicitly resolve them. Furthermore, Grell et al. (2013) have found that letting the model explicitly resolve mesoscale processes can frequently not be enough to neutralize the moist instability, leading to an incorrect representation of tropical cyclones (TCs). Therefore, there are continuing efforts to adapt the parameterizations to these resolutions, as

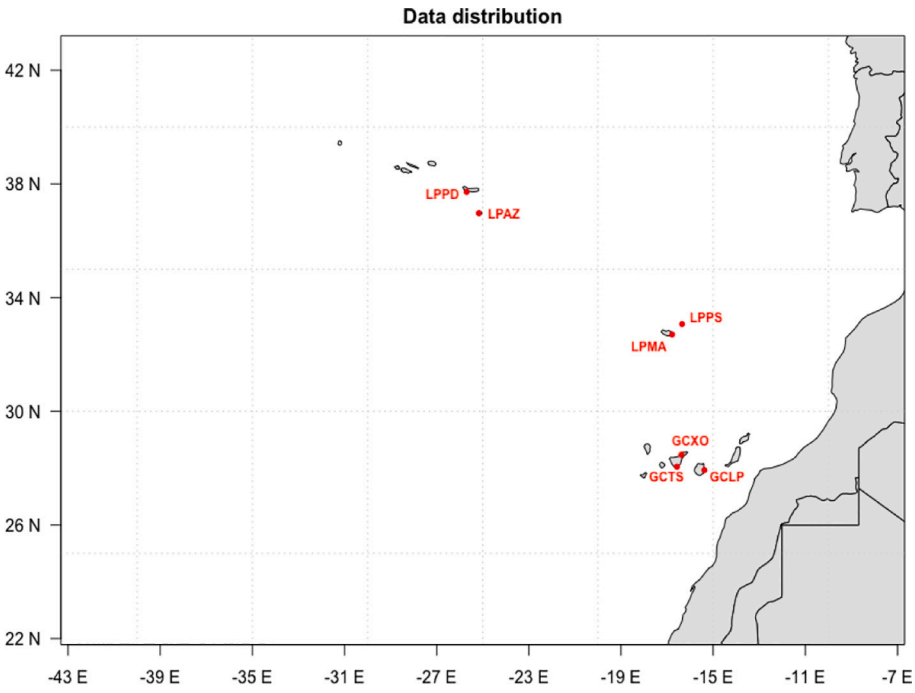

Fig. 1. Domain of simulation. Red dots show the location of the available airports with the METAR and sounding data.

those by Grell and Freitas (2013) who created a new CP able to remove moist instability and to present a stronger model convergence for TC intensity (Sun et al., 2014). Other works show that this scheme carries out smoother transitions when simulating cloud-scale processes as resolution increases (Arakawa et al., 2011; Arakawa and Wu, 2013). Despite this, it was decided to use the WRF User Guide 4.0 physics configuration for this case study (where the cumulus scheme is not considered for resolutions lower than 12 km), as this is the standard recommended by the model developers. Finally, the initial/boundary conditions are obtained from the Integrated Forecasting System (IFS) analysis of the National Meteorological Archival and Retrieval System (MARS) of the ECMWF with a 0.25° horizontal resolution every 6 h.

The HARMONIE model configuration (v40h1.1.1 version in this study) resembles WRF's one as much as possible to maintain the consistency of the study. Defined with the HARMONIE default physics options (Bengtsson et al., 2017), the model also has a main domain with 2.5 km resolution and the same grid dimensions in the west-east and south-north directions, although in this case, the model has 65 hybrid sigma-pressure levels in the vertical. The initial/boundary conditions are the same as those used for WRF. In this case, the model is configured with a temporal resolution of 75 s (Bengtsson et al., 2017). Operated at 2.5 km resolution this model has a convection-permitting configuration and uses a non-hydrostatic spectral dynamical core with a semi-Lagrangian and semi-implicit discretization of the equations. In this way, more realistic results are obtained (Bengtsson et al., 2017) compared to other models, which may provide an added value to the study of tropical transitions, such as the STC events. Both model domains correspond to the area depicted in Fig. 1.

2.2. METAR and soundings

A set of available observational Meteorological Terminal Aviation Routine Weather Reports (METAR) from six different airports are used for the analysis: two airports from the Canary Islands (GCLP and GCTS, as per ICAO codes), two from Madeira archipelago (LPMA and LPPS) and two from Azores (LPAZ and LPPD). It has to be remarked that during the event only a single sounding from Tenerife-Norte (GCXO) airport produced valid observations in the domain of study, most probably due to the meteorological conditions rendering the rest of them useless. The available METAR and sounding data distribution are shown in Fig. 1.

2.3. MSG-SEVIRI

The SEVIRI is the main instrument of the MSG geostationary satellites which are operated by the European Organisation for the Exploitation of Meteorological Satellites. SEVIRI provides image data in four Visible and Near-Infrared (VNIR) channels and eight IR channels (ranging from 3.9 to 13.4 μm), providing continuous precise data throughout the atmosphere, which enhances the quality of the initial and boundary conditions for NWP models (Pasternak et al., 1994). The eight IR channels, located in the thermal region, provide, among other, cloud, land, and sea surface temperature data. With a temporal resolution of one hour, the horizontal resolution for the standard channels is 5 km, except for the High-Resolution Visible (HRV) channel which has a sampling distance at the nadir of 1 km. This channel can be a useful tool to better identify the onset or end of severe events, such as STCs.

These products are used in this study to validate the WRF and HARMONIE outputs using the BT field, as suggested by Bormann et al. (2014) and Otkin et al. (2009). Moreover, the 8.7 μm, 10.8 μm, and 12.0 μm IR channels are the suitable ones to distinguish the top cloud cover and surface temperatures. According to several authors (Zingerle, 2005; Bormann et al., 2014; Montejo, 2016), the 10.8 μm and 12.0 μm IR channels turn to be especially sensitive to the existence of clouds since they correspond to the IR atmospheric window. Also, these IR channels are considerably more precise in detecting the cloud vertical distribution and some surface features, such as temperature or emissivity (Chevallier and Kelly, 2002). Therefore, the 10.8 μm long-wave IR channel is selected in this study as observational data.

2.4. Methodology

In order to carry out a validation against several observations (airport METAR, sounding, and BT data) of the WRF and HARMONIE models, a point-to-point validation is firstly performed by analyzing the available METAR results of six different airports with both models outcomes using the closest model grid point to the observation location.

For this, some simulated variables (2 m temperature, 2 m dew-point temperature, and 10 m wind speed) are assessed every three hours at each airport. Furthermore, the vertical structure of the atmosphere is analyzed using the temperature and wind speed of a meteorological sounding.

The MSG-SEVIRI products are also used to validate the WRF and HARMONIE simulations. The methodology described by Otkin and Greenwald (2008) and Bormann et al. (2014) is used here for both model simulations. In order to establish the realism of the cloud distribution, the BT frequency distribution is used (Bormann et al., 2014), depicted for models and satellite observations, allowing to evaluate the capacity of both models to capture the quantity and altitude of clouds. Following the methodology described by López et al. (2007), Aznar et al. (2010), Loew et al. (2017), Díaz-Fernández et al. (2020), and WWRP (World Weather Research programme) and WGNE (Working Group on Numerical Experimentation) Joint Working Group on Forecast Verification Research (2017), an analysis has been assessed through several skill scores. These skill scores have been determined for every grid point of the domain for both analyzed dates (pre-STC and STC stages). Spatial averages of these scores are provided to summarize the information into a single coefficient. The skill scores used in the current paper are defined as follows:

❏ *Linear product-moment correlation coefficient of Pearson (R):*

$$R = \frac{\sum_{i=1}^{N}\left(BT_{s,i}\underline{BT}_{s,i}\right)\left(BT_{o,i}\underline{BT}_{o,i}\right)}{\sqrt{\sum_{i=1}^{N}\left(BT_{s,i}\underline{BT}_{s,i}\right)^2}\sqrt{\sum_{i=1}^{N}\left(BT_{o,i}\underline{BT}_{o,i}\right)^2}}$$

where BT_s and BT_o are simulated and observed BT, respectively, for every time step and specific grid point.

❏ *Relative BIAS (hereafter bias):*

$$BIAS = \frac{\sum_{i=1}^{N} BT_{S,i}}{\sum_{i=1}^{N} BT_{O,i}}$$

❏ *Root-mean-square error (RMSE):*

$$RMSE = \sqrt{\left(\frac{(BT_s - BT_o)}{N}\right)^2}$$

where N is the total number of time steps.

❏ *Mean absolute error (MAE):*

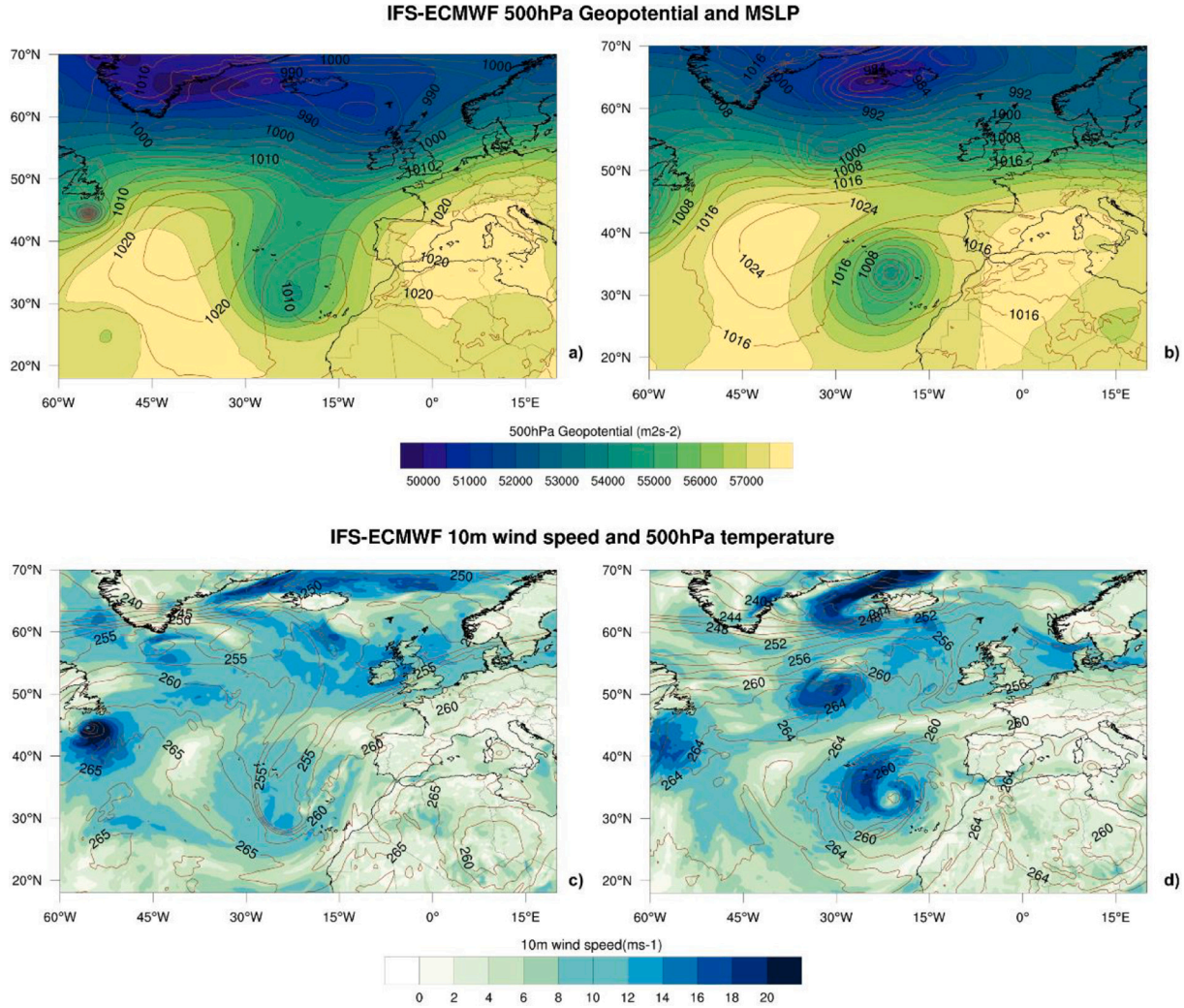

Fig. 2. Mean sea level pressure (hPa, contours) and 500 hPa geopotential height (m, shaded) at a) 19 and b) 20 October 2014 at 1800UTC. 10 m wind speed (m/s, shaded) and 500 hPa temperature (K, contour) at c) 19 and d) 20 October 2014 at 1800UTC.

$$MAE = \frac{\sum_{i=1}^{N}\left(BT_{s,i} - BT_{o,i}\right)}{N}$$

❑ *Standard deviation (SD):*

$$SD = \frac{\sqrt{\sum_{i=1}^{N}\left(BT_i - \underline{BT_i}\right)^2}}{N}$$

3. Results and discussion

Before showing the results the synoptic situation of the event is briefly described below to know the environment in which the cyclone formed and intensified. During the formation of this meteorological event, several atmospheric processes were involved. It is remarkable the highly meridional atmospheric circulation over the Eastern North Atlantic, characterized by an outstanding undulation in the geopotential field (Fig. 2a). The associated deep trough dug into subtropical latitudes at the beginning of day 19 October. This trough in conjunction with a low-level baroclinic zone favored the genesis of a weak extratropical cyclone to the northwest of the Canary Islands by quasigeostrophic (QG) forcing. By October 20 (Fig. 2b), the cyclone is no longer supported by QG forcing and begins to be governed by diabatic processes that would help its intensification. By this time, the cyclone cut off, isolated and rapidly deepened. Moreover, this rapid intensification is most likely to have been caused by the intense latent heat released, which promoted a powerful circulation within the center of the cyclone leading to strong winds and precipitation (Quitián-Hernández et al., 2020).

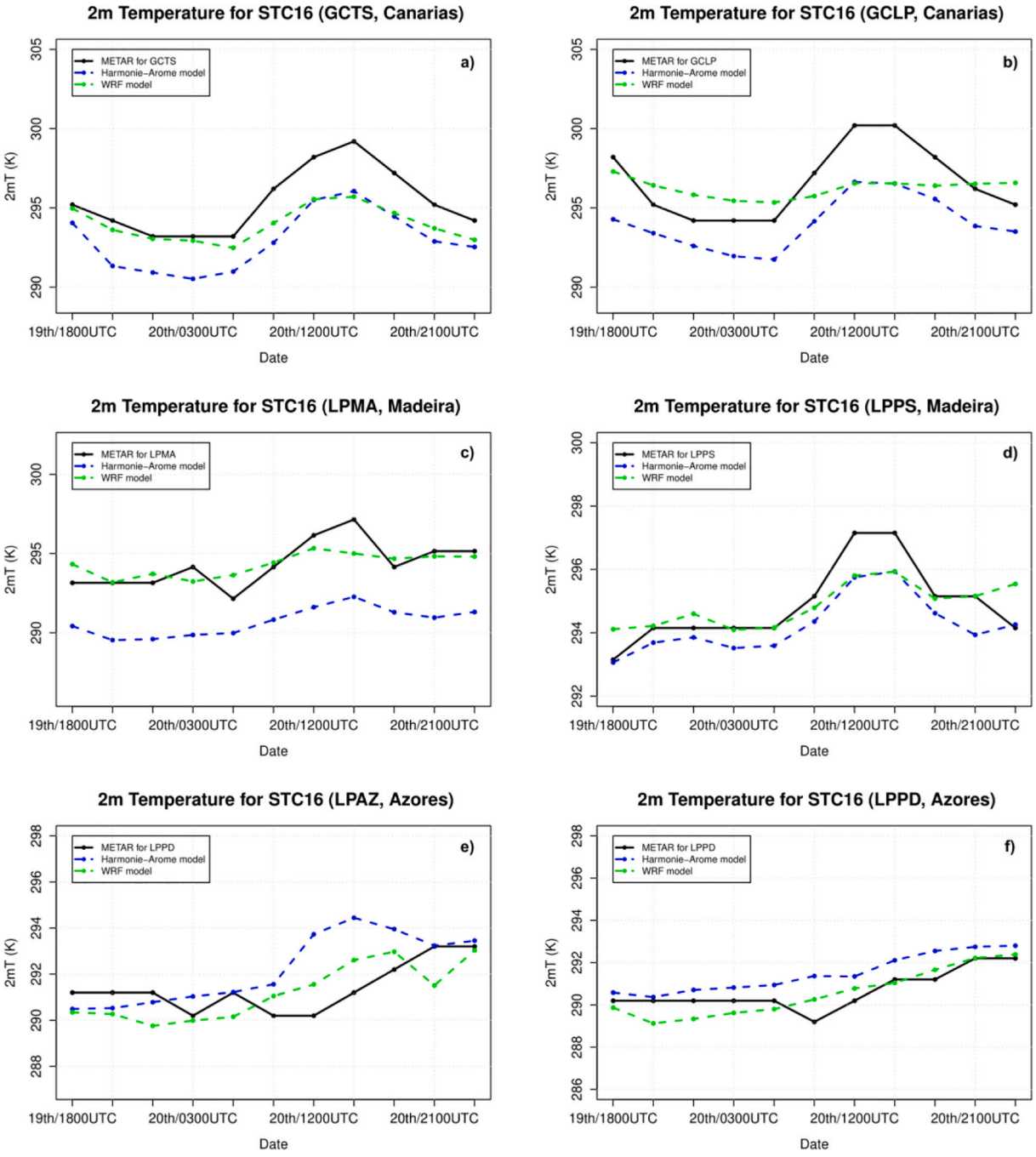

Fig. 3. Temporal evolution of 2 m temperature for a) GCTS, b) GCLP, c) LPMA, d) LPPS, e) LPAZ and, f) LPPD airports.

Moreover, regarding the 10 m wind speed field (Fig. 2c and d) it is outstanding the increase in the values once the cyclone has rapidly intensified (Fig. 2d), being notable a boost of them in the northwestern area of the cyclone. These results are related to a Shapiro-Keyser development which, in conjunction with the upstream deep convection, favored the intensification of the low-level winds in that area (Quitián-Hernández et al., 2020). Furthermore, concerning the 500 hPa temperature (Fig. 2c and d) it is noteworthy the higher values located at the center of the cyclone once it has intensified (Fig. 2d). These results are again related to a Shapiro-Keyser configuration that underwent a warm seclusion process. (More information about this configuration can be found in Quitián-Hernández et al. (2020).

Once the synoptic framework in which the cyclone is developed has been established, simulations of the WRF and HARMONIE models versus observational data will be compared. To do this, a three-ways analysis is carried out to obtain a more complete appraisal of the results. Firstly, a validation against surface observations is assessed in Section 3.1 by selecting the closest spatial points to the airport METAR data. A complete analysis of the cyclone evolution is carried out, emphasizing on the pre-STC and pure-STC dates. Secondly, a vertical analysis is evaluated in Section 3.2 by means of a sounding in the only available station for the only available hours: 20 October 2014 at 0000 UTC (still considered pre-STC according to the CPS results, see Quitián-Hernández et al., 2020) and 1200 UTC (pure-STC). Finally, BT spatial and cloud top distributions are analyzed in Section 3.3 using several skill scores to evaluate the model performance and skillfulness.

3.1. Validation against surface observations

In this subsection, a validation of the simulated WRF and HARMONIE variables against METAR observations is presented. On every panel of each figure of this section, the blue lines correspond to the HARMONIE model simulation, the green lines to the WRF model simulation, and the black lines to the METAR data.

Regarding the 2 m temperature outcomes for the Canary Islands area, it is remarkable the similarity in the behavior of both models with the METAR data in GCTS (Fig. 3a), being the WRF model the one with better results. In addition, during the first hours of simulation (pre-STC period), the WRF model was particularly consistent with the observations. The HARMONIE model shows a similar behavior compared to the METAR data, despite the observed general underestimation in both airports analyzed (Fig. 3a and b). However, the WRF outputs for GCLP (Fig. 3b) show a temperature too stable. Fernández-González et al. (2019) carried out a validation of several fog episodes in Tenerife-Norte airport (GCXO) using both WRF and HARMONIE models. In this study, several variables related to fog formation and diffusion were tested and, among them, the temperature, dew-temperature, and wind speed near the surface. Analyzing the results for the temperature, it is remarkable that both models underestimated the values, which is consistent with what is obtained in the current study in the Canary Island area. However, Fernández-González et al. (2019) concluded that better outputs were found by the HARMONIE model compared to the WRF model, which cannot be inferred in this analysis as the HARMONIE model showed a greater underestimation. This could be due to an exhaustive assimilation process carried out in the Fernández-González et al. (2019) study for the HARMONIE model. Nevertheless, the results obtained in the current study for the HARMONIE model are in agreement with the 2 m temperature verification carried out by the HIRLAM consortium (Santos-Muñoz, 2015). It should be reminded that the HIRLAM consortium verifications are here taken as a reference for validating the outcomes of this work due to the scarce literature relative to the STC's study with the HARMONIE model.

The 2 m temperature outcomes of the Madeira Islands area (Fig. 3c and d) show a general underestimation by the HARMONIE model in comparison to the observations, being the WRF model the one with better simulations in LPMA (Fig. 3c). Concerning LPPS (Fig. 3d), it is noticeable the consistency of both models. However, during the pre-STC stage, while the WRF model shows a slight overestimation, the HARMONIE model shows a slight underestimation. During the pure STC period, it was the WRF model that underestimated the results the least. Furthermore, considering the HIRLAM verification (Santos-Muñoz, 2015) a slight underestimation of the HARMONIE results in the Madeira Islands area is obtained.

The simulations of the Azores Islands area (Fig. 3e) show a good 2 m temperature simulation in LPAZ with both models during the pre-STC period. However, during the pure-STC stage, it is noteworthy a general overestimation of both models, being slightly lower for the WRF model. Regarding LPPD (Fig. 3f), it is worth highlighting the consistent outputs of both models compared to the METAR data, showing a very similar behavior during the whole simulation. A slight overestimation is found in the middle of the simulation (from 0600UTC to 1800UTC on the 20th), being the WRF model the one with better outcomes. In this case, there is no available HIRLAM verification for the Azores Islands area to sustain the HARMONIE results.

In general terms, the WRF model shows better 2 m temperature results. However, its behavior turns out to be flatter compared to the observations. The HARMONIE model shows, in every analyzed area, a greater bias. However, its behavior is remarkably similar to the observations. Furthermore, it is outstanding the underestimation found in both, the Canary and Madeira Islands area, which are located just below the cyclone cold front during the pre-STC stage. This negative bias is sustained by several works (Hu et al., 2010; Avolio et al., 2017), where cold biases were also found in a temperature WRF sensitivity analysis during the daytime. Besides, during the pure-STC stage, the WRF model shows a greater bias even though there is less influence of the cyclone. On the other hand, it is noteworthy the general overestimation found in the Azores Islands area, located to the NW of the cyclone. Moreover, the Azores Islands is the only area where the HARMONIE simulation shows a lower bias during the pre-STC stage. This could be due to the fact that there was no cyclone influence in the Azores area during that period. Once the cyclone begins to acquire subtropical characteristics, it is noticed a greater bias from both models.

The 2 m dew-point temperature outcomes in the Canary Islands area (Fig. 4a) show a general underestimation from both models in GCTS, being the HARMONIE model, the one with better results. In addition, the WRF underestimation is also supported by Avolio et al. (2017) where colder biases are obtained for a near-surface temperature analysis, among other variables. Regarding the simulations in GCLP (Fig. 4b), it is remarkable a slight overestimation by means of both models, being again the HARMONIE model, the one with better outputs compared to the observations. Nevertheless, despite the observed bias, it is outstanding the similar behavior found for both models compared to the METAR data. Under the validation by Fernández-González et al. (2019), it is also found a negative 2 m dew-point temperature bias in Tenerife Island but to the south (GCTS) in the current study. Besides, it is worth noting a light underestimation (overestimation) in GCTS (GCLP) although the HIRLAM consortium verification offers overestimation (underestimation) in such zones (Santos-Muñoz, 2015).

Evaluating the simulations in the Madeira Islands area (Fig. 4c and d), it is noticed a similar behavior by both models. However, while the WRF model shows a positive bias in LPMA airport (Fig. 4c), it slightly underestimates in LPPS airport (Fig. 4d). The depicted underestimation by WRF in LPPS, also obtained for the 2 m temperature, is sustained by Avolio et al. (2017). Besides, the HARMONIE model shows again a general underestimation in both airports. Moreover, considering the HIRLAM verification (Santos-Muñoz, 2015) it is found a general underestimation, confirming the consistency of the HARMONIE simulations in both airports (Fig. 4c and d). All in all, for the Madeira Islands area, WRF is the one with slightly better outcomes compared to the observations.

The 2 m dew-point temperature results in the Azores Islands area (Fig. 4e and f) show a general overestimation and very similar behavior

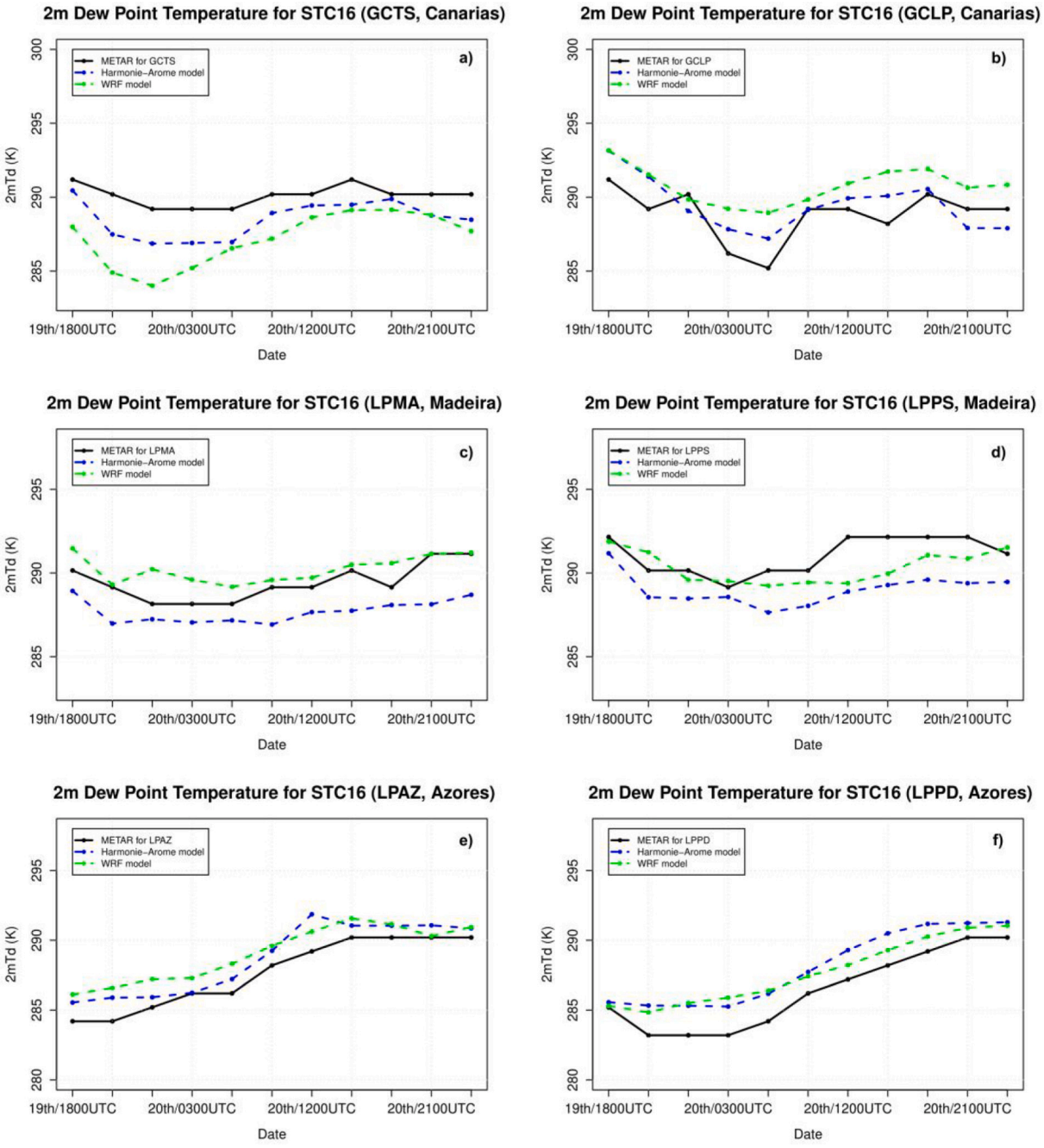

Fig. 4. Same as Fig. 3 except for 2 m dew-point temperature.

by both models compared to the METAR data. Concerning the simulations in LPAZ, similar results are found by both models, showing the HARMONIE model slightly better results during the pre-STC period. However, the WRF model is the one with slightly better outputs in LPPD (Fig. 4f). As occurred for the 2 m temperature validation there is no available HIRLAM verification for the Azores Islands area to sustain the HARMONIE outcomes.

On the whole, the HARMONIE model shows a minor 2 m dew-point temperature general underestimation in the Canary and Madeira Islands, except in the GCLP area where it overestimates. Besides, the HARMONIE model shows better outcomes for the Canary Islands compared to the WRF model. Additionally, despite the slight overestimation found in the Madeira area, the WRF model is the one with better outputs. Furthermore, there was no complete concordance in the HARMONIE simulations in the Canary and Madeira Islands when considering the HIRLAM verification results. Moreover, the positive bias noticed in the Azores area for the 2 m temperature is again noticed in the 2 m dew-point temperature. Besides, the latest version available of the HARMONIE at the time of the study (v40h1.1.1) has been used for this work. According to the HIRLAM consortium coordinator, this last version may have introduced some bias in the area which is being addressed in the following version (Santos-Muñoz, 2015).

The 10 m wind speed outcomes for the Canary Islands area (Fig. 5a) during the pre-STC stage in GCTS show a general overestimation by both models, even though the HARMONIE model is the one with slightly better results. Moreover, during the pure-STC period, both models slightly underestimated, being this time the WRF model the one with better outputs. This could be due to the intense convective processes that take place during the pre-STC period, which could induce a greater instability in the model simulation that contributes to bigger errors.

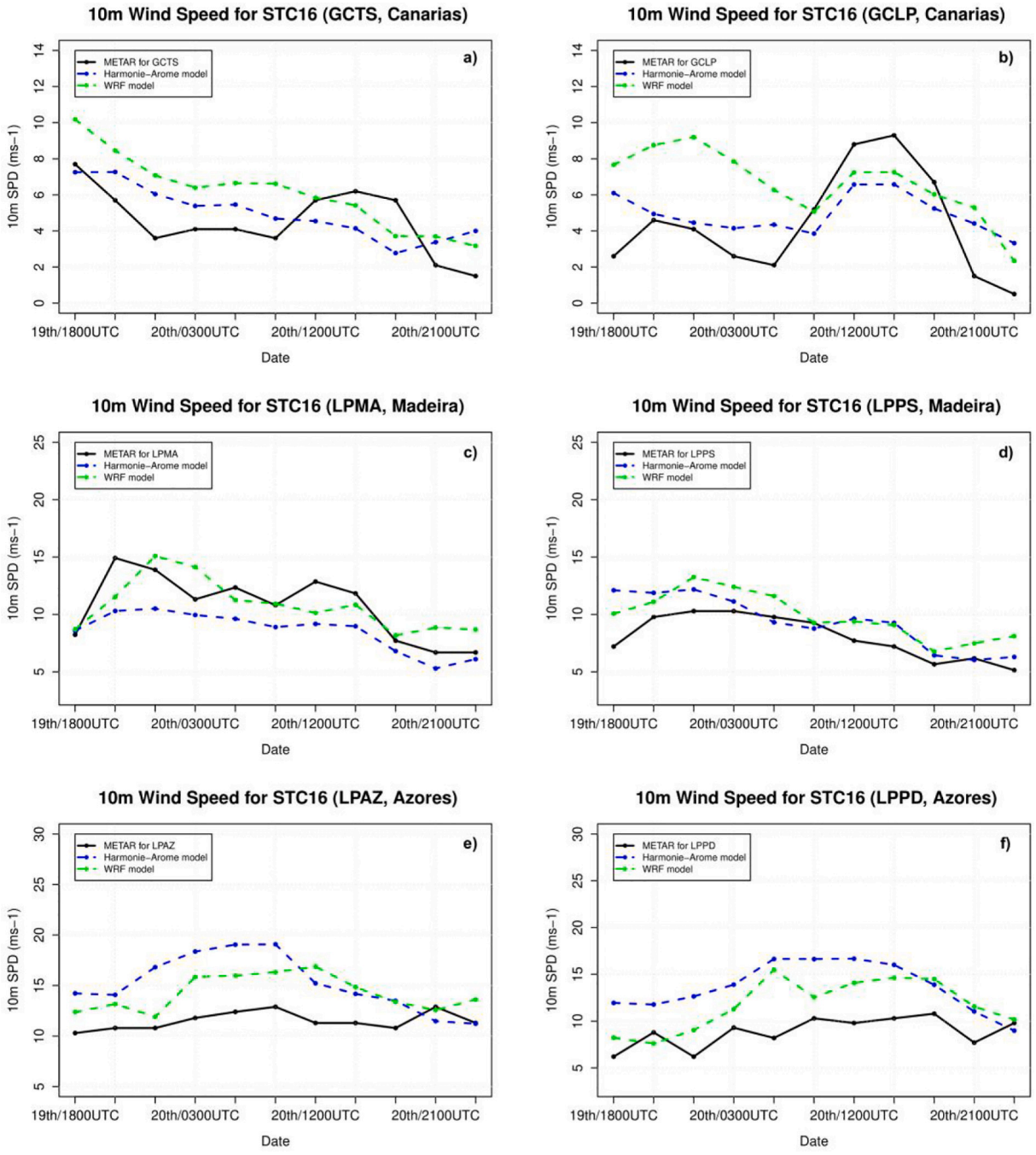

Fig. 5. Temporal evolution of 10 m wind speed for a) GCTS, b) GCLP, c) LPMA, d) LPPS, e) LPAZ and, f) LPPD airports.

Furthermore, the simulations for GCLP (Fig. 5b) during the pre-STC stage showed that, despite a positive bias being found for both models, the HARMONIE simulation showed a more consistent behavior and better results compared to the observations. During the pure-STC period, a negative bias was found for both models in the GCLP area. In this stage of the cyclone development, the WRF model shows more coincident outcomes with observations. Regarding Fernández-González et al. (2019) results, the HARMONIE model tends to overestimate wind speed in the Tenerife area. These outputs are in concordance with the obtained results of the current work, where the HARMONIE generally overestimates in the Canary Islands area (Fig. 5a and b). Additionally, better outcomes for the wind speed are obtained with such model in Fernández-González et al. (2019), which again sustain the results here obtained.

The 10 m wind speed for the Madeira Islands area (Fig. 5c) shows a very similar behavior by both models in LPMA, noticing better outcomes at the beginning and the end of the simulation. Concerning LPPS (Fig. 5d), both models overestimate, being the HARMONIE model the one with more consistent behavior and slightly better results compared to the METAR data.

The 10 m wind speed outputs for the Azores Islands area (Fig. 5e) show a general overestimation by both models becoming subtle at the end of the simulation in LPAZ. They both display a similar behavior, showing the WRF model better results over almost the entire life cycle. Something similar happens for the LPPD airport (Fig. 5f), except for some instants of the cyclone life. In this case, there are no HIRLAM verifications for 10 m wind speed available to support the HARMONIE simulation. However, it can be concluded that both models show very

similar outcomes in each airport not being possible to infer which one is the best simulating this field.

All in all, a general overestimation is observed for the wind speed in all the analyzed airports. These results are supported by Avolio et al. (2017) where it is concluded that a positive bias is usually found by the WRF model when simulating the 10 m wind speed. Furthermore, according to Lamraoui et al. (2018), larger biases of WRF simulated 10 wind speed could be due to the absence of necessary space and time that facilitate a correct forcing from the boundary condition towards a balanced solution. This could be the reason for the WRF general wind speed overestimation found in the current study.

Regarding the two model results, it cannot be determined that one model prevails over the other in terms of accuracy. Focusing on each analyzed variable, while better results are obtained by WRF for the 2 m temperature analysis, similar results are obtained by both models for the 2 m dew-point temperature and 10 m wind speed analysis. Moreover, considering the area of study, HARMONIE performs slightly better for the Canary Islands area compared to the WRF model that shows slightly better results for the Madeira and Azores area.

3.2. Soundings

In order to carry out a vertical analysis of the atmosphere during the genesis and intensification of the system, the only available sounding (GCXO) in the study area is examined. The temperature (Fig. 6) and wind speed (Fig. 7) outcomes are depicted. Focusing on the temperature results, it is remarkable for the two available dates (20 October 2014 at 0000 UTC (pre-STC) and 1200 UTC (pure-STC)) the good results of both models throughout the entire temperature evolution (Fig. 6a and b) concerning the sounding observations (black line). Regarding the BIAS

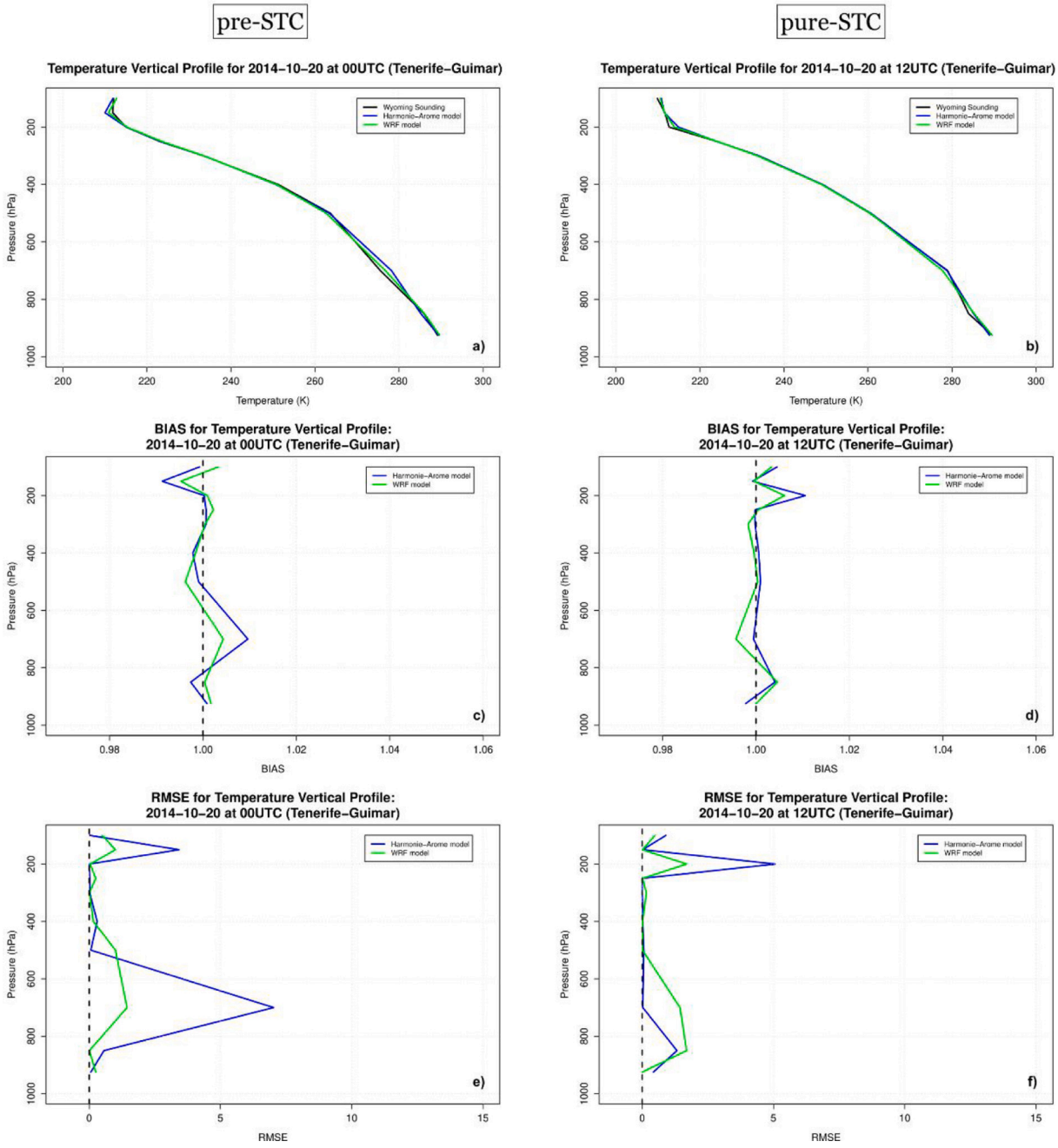

Fig. 6. a), b) Temperature vertical evolution, c), d) BIAS and e), f) RMSE results for 20 October 2014 event at 0000 UTC (left) and 1200 UTC (right) for GCXO-Tenerife Norte airport.

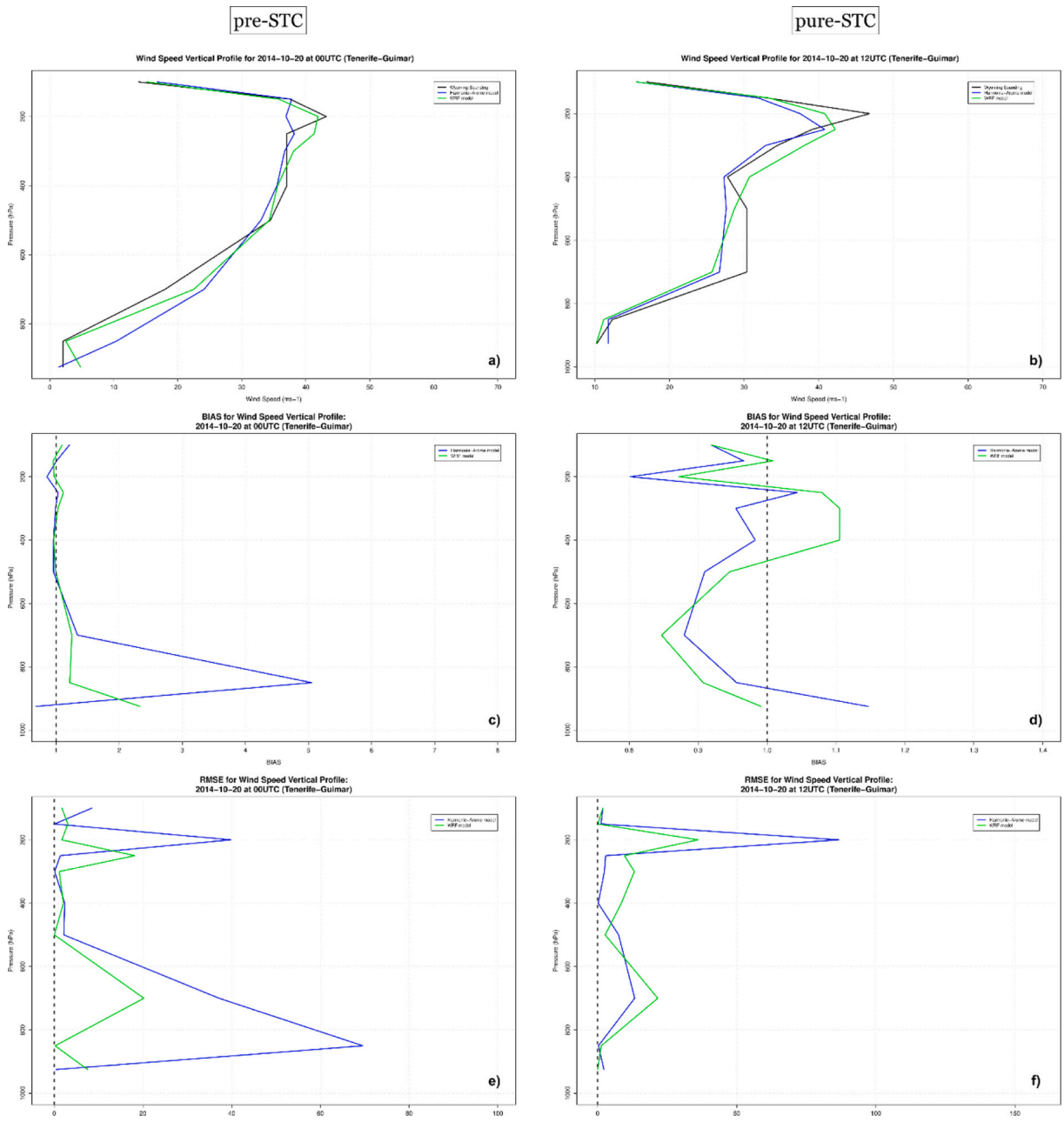

Fig. 7. Same as Fig. 6 except for wind speed vertical evolution.

(Fig. 6c and d) results for both analyzed dates, it is noticeable the general consistency and similar behavior of both models, being the WRF model (green line) the one with slightly better results in comparison to the HARMONIE model. In regard to the RMSE (Fig. 6e and f) results, it is remarkable the good results of the WRF model compared to HARMONIE. Furthermore, the outputs by both models during the pure-STC period turn out to be slightly better than the obtained during the pre-STC period. This could be due to the mitigation of the convective processes once the cyclone is formed, which on the contrary could lead to the model instability and therefore to produce bigger errors (Zhang et al., 2007; Hohenegger and Schär, 2007; Weisman et al., 2008; Uboldi and Trevisan, 2015). Moreover, it is remarkable the higher errors found in the mid-troposphere during the pre-STC period. According to several studies (Kanase and Salvekar, 2014; Kanase and Salvekar, 2015; Hazra and Pattnaik, 2020), there is a remarkable influence of the WRF YSU PBL parameterization schemes over the essential atmospheric variables, such as temperature, moisture or wind, being directly associated with deep convection. In relation to this fact, the above-mentioned authors observed that the YSU scheme produces a warm bias in the middle troposphere, which results in higher latent heat flux (and so, a higher convective instability and greater cyclone intensity), which would explain the higher temperatures in the middle troposphere (up to 600 hPa) that have been obtained in the current study.

Regarding PBL, both models showed a slight underestimation during the pre-STC stage and a small overestimation during the purely-STC period. According to Hu et al. (2010) and Hariprasad et al. (2014) the WRF YSU PBL generates greater temperatures in the lower troposphere, which sustain the obtained WRF outcomes. According to the HIRLAM consortium (Santos-Muñoz, 2015), coherent results are obtained with the HARMONIE model near the surface for the pre-STC stage. However, during the pure-STC stage, the HIRLAM verification presents a negative bias (Santos-Muñoz, 2015) around the PBL while the HARMONIE simulation slightly overestimates.

On the other hand, the BIAS and RMSE obtained for the tropopause

(around 200 hPa) for both models show a similar behavior, being the WRF model the one with slightly better results compared to HARMONIE. Moreover, while both models show an underestimation during the pre-STC stage, larger values are shown during the pure-STC period. According to the HIRLAM verification (Santos-Muñoz, 2015), it can be remarked the coherence of the obtained HARMONIE outputs when simulating the temperature at the tropopause for both dates.

An overestimation of the wind speed in the PBL for the pre-STC period (left side of Fig. 7) can be noted for both models' outcomes, showing the best results located in the mid-troposphere (from around 700 hPa upwards). Besides, the found wind overestimation is in concordance with the almost general overestimation attained during the pre-STC period at practically all the analyzed airports (Fig. 5). According to Hayashi et al. (2008), Shimada et al. (2011) and, Kanase and Salvekar (2014), positive biases are obtained near the surface when simulating wind speed profiles with the YSU PBL parameterization scheme, which supports the obtained WRF outputs. Moreover, the obtained HARMONIE outcomes for both STC dates in the lower atmosphere are coherent with a positive wind speed bias of the HIRLAM verification results near the surface (Santos-Muñoz, 2015). Furthermore, the mid-troposphere results during the pre-STC stage show a large coincidence between the two models. Besides, the RMSE outputs (Fig. 7e) show higher errors for both models in the PBL and the tropopause, with a slight deviation between them but showing the WRF model better results in comparison to HARMONIE. In the pure-STC stage (right side of Fig. 7), it can be noticed a slightly better behavior by the HARMONIE model compared to the sounding, with a general underestimation during practically the whole profile. In addition, the RMSE outputs (Fig. 7f) show slightly better results for WRF in the PBL and mid-troposphere compared to HARMONIE.

Concerning the tropopause (around 200 hPa) outcomes and both analyzed periods, the WRF model tends to underestimate the wind speed, in contrast to the temperature results. Moreover, the RMSE outputs for WRF during the pre-STC (Fig. 7e) and pure-STC period (Fig. 7f) are again smaller than the obtained by HARMONIE, although these HARMONIE simulations are in agreement with the verification results made regularly by the HIRLAM consortium.

3.3. Spatial distribution

In this subsection, a comparison of the BT frequency distribution simulated by the WRF and HARMONIE models and the one observed by the MSG-SEVIRI satellite is assessed (Fig. 8). Simulated BT spatial distributions for both analyzed dates are additionally presented (Fig. 9).

Analyzing the BT frequency distribution for the pre-STC stage (Fig. 8a), the observation results should be first noted. The MSG-SEVIRI presents a major concentration around 293 K, showing that most temperatures detected correspond to low clouds or terrain, with a sharp decrease to higher temperatures and a smooth transition to lower temperatures. An asymmetrical distribution is thus observed with a long tail extending to 210 K, indicating presence of high-level cloudiness. The

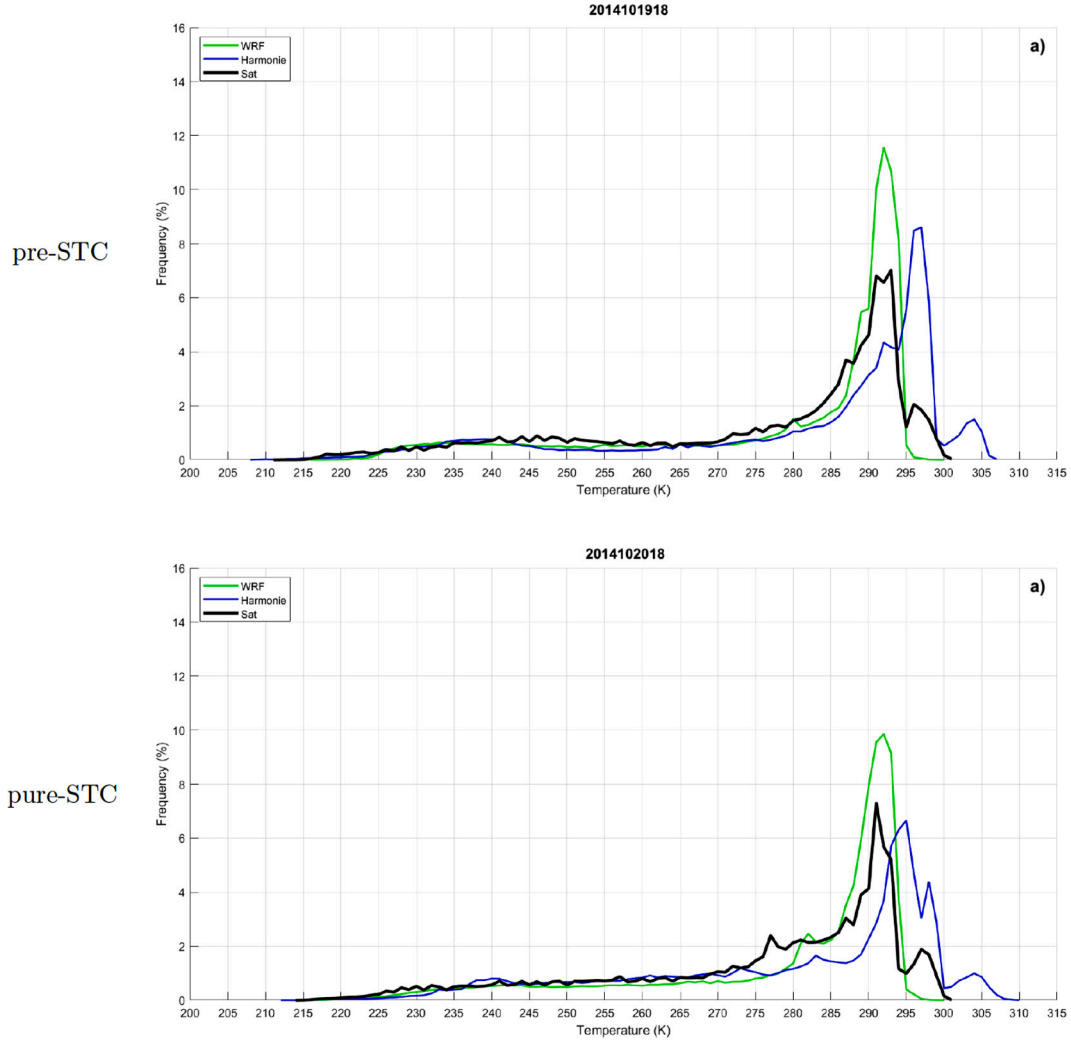

Fig. 8. Frequency distribution (%) of BT (K) for the observed MSG-SEVIRI and the WRF and HARMONIE models for a) 19 and b) 20 October 2014 at 1800UTC.

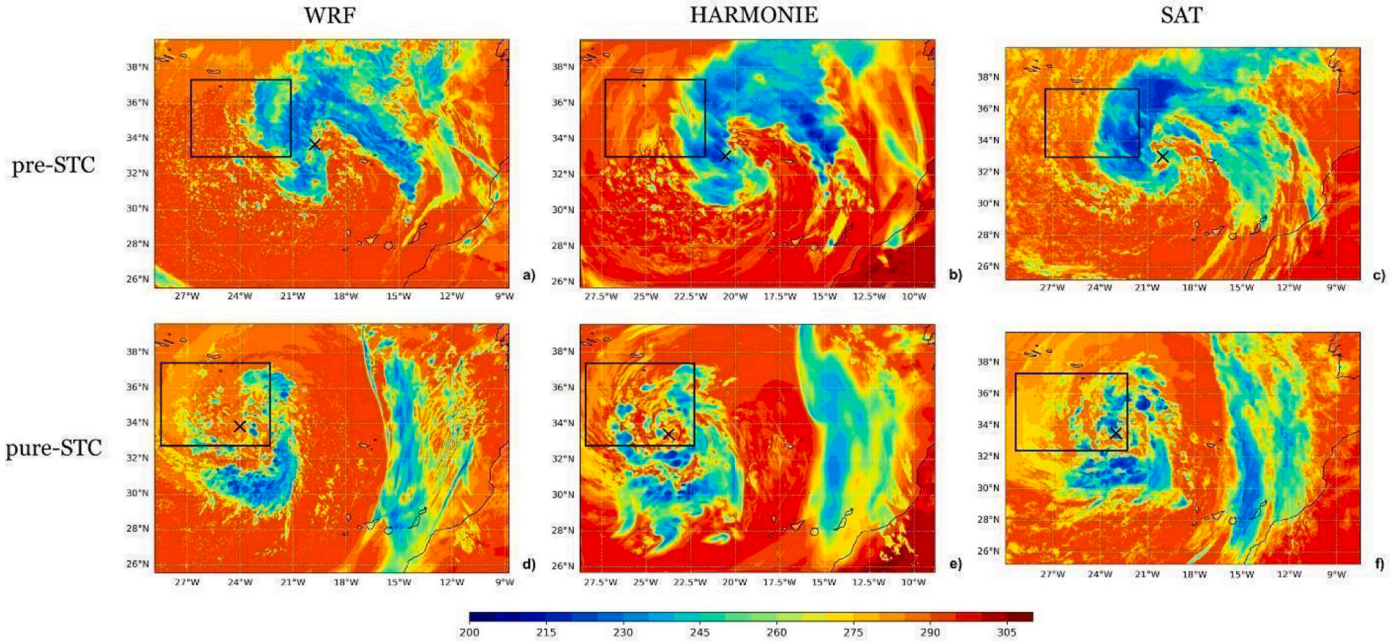

Fig. 9. BT (K) spatial distribution for the a), d) WRF model, b), e) HARMONIE model, and c), f) MSG-SEVIRI satellite for 19 (top) and 20 (bottom) October 2014 at 1800 UTC. Black rectangles delimit the Shapiro-Keyser structure. Black cross depicts the center of the STC.

MSG-SEVIRI distribution shows a wide range of altitudes of the observed clouds.

The WRF BT frequency shows an asymmetrical leptokurtic distribution towards higher BTs and indicating simulated low cloudiness. These WRF results are consistent with those found in Shi et al. (2018) and Jankov et al. (2011), where greater values of simulated BT were obtained compared to observations. In Shi et al. (2018), simulated BT was compared to China's geostationary satellite (FY-2D), whereas in Jankov et al., 2011it was evaluated against GOES-10 imagery, being the main goal of these studies to evaluate the importance of synthetic satellite images to carry out an appraisal of the model's efficiency. Regarding the WRF results in the frequency distribution, the outcomes show that WRF tends to simulate a continuous distribution of clouds, with a particular overestimation in 290 K. However, while WRF well-simulated the mode temperature (centering of the peak), it overestimated the frequency. On the other hand, the HARMONIE BT frequencies are slightly closer to the observed frequency distribution in the pre-STC stage, showing in general a similar behavior compared to observations, albeit a 5 K bias to higher BTs and a slight underestimation of the quantity. Moreover, the higher BTs obtained is consistent with the overestimation found in the 2 m dew-point temperature field for the Canary Islands' GCLP airport (Fig. 4b) and Azores area (Fig. 4e and f) and at the surface of the temperature sounding (Fig. 6b).

Regarding the pure-STC period frequency distribution (Fig. 8b), WRF and HARMONIE models present similar behaviors to those described before. Again, and despite the already observed deviation to higher BTs, the HARMONIE distribution is more consistent with the observations, showing similarly the two peaks at higher BTs (295 and 305 K) in this cyclone stage in accordance to the MSG-SEVIRI results. The WRF model also shows a slight deviation to higher BTs at the peak frequency. These results confirm the ability of both models to reproduce quite well the cloudiness and height of clouds during the formation of the cyclone. Moreover, for the pure-STC stage, the observed low-level clouds overestimation is compatible with the overestimation found in the 2 m temperature for the Azores area (Fig. 3e and f), in the 2 m dew-point temperature for the Canary Islands' GCLP airport (Fig. 4b) and Azores area (Fig. 4e and f), and at the surface of the temperature sounding (Fig. 6e). Consequently, the Azores area shows, in general, a remarkable overestimation of several variables that could be related to the warm bias found in the BT frequency distribution graph.

The spatial BT fields for the two selected dates (Fig. 9) show good results with the HARMONIE model (Fig. 9b and e) compared to the observations (Fig. 9c and f). Furthermore, the higher BT values found in the vicinity of the cyclone are consistent with the bias obtained for this model on the frequency distribution (Fig. 8). Moreover, it is remarkable the overestimation of BT values found for the WRF model when simulating middle and lower clouds (yellow and red tones, Fig. 9a, d). Furthermore, there is also an overestimation of cloud tops (blue tones), particularly in the cold front area during the pre-STC period. According to Otkin and Greenwald (2008), the PBL and microphysics schemes wield a notable influence on the cloud spatial distribution. Indeed, the current results are in agreement with those obtained by those authors where simulations employing the YSU PBL scheme could generate a larger amount of upper-level clouds. Moreover, this PBL scheme in conjunction with the WSM6 microphysics scheme could generate fewer upper-level cloud tops, and so, a larger amount of cloudless areas between convective cells. This is reflected in the red tones also found in the surroundings of the cyclone for WRF, which are in agreement with the displayed overestimation of high BT (293 K) on the frequency distribution graph (Fig. 8). Besides, it is remarkable the more dispersed/heterogeneous upper level clouds distribution simulated by the WRF model, leading to a lower precision and realism. It is clear that it does not capture really well the upper altitude cloudiness and overestimates the lower clouds. On the other hand, the HARMONIE model outcomes are slightly more consistent with the observations, even considering that the surface and cloud tops temperatures are higher than observed, as already seen in the frequency distribution bias. In addition, it is outstanding the well-defined cumulus located around the center of the cyclone simulated by the HARMONIE model, similar to those observed, and the transitions to the outer limits of the domain, especially on the pure-STC stage (Fig. 9e).

To end the spatial distribution assessment, the Shapiro-Keyser structure (Shapiro and Keyser, 1990) is also evaluated, as done in Quitián-Hernández et al. (2020). The surface heat fluxes and strength of this area (black rectangles in Fig. 9) is directly related to the convective processes developed around the northwestern area of the cyclone, which plays a key role for its intensification and development into STC. Once again, it can be seen that the scattered structure of the WRF simulation

produces poor results. The slight absence of upper-level clouds, especially for the pre-STC stage, hinders the results. Also, in the pure-STC outputs we can find an overestimation of low-level cloudiness, and so, clearer areas than observed. On the contrary, HARMONIE produces suboptimal but realistic results. In the Shapiro-Keyser area the model clearly shows a warm bias, generating fewer and lower clouds than observed, but presenting a much more realistic structure and distribution of BT.

Regarding the analysis carried out employing several skill scores, it can be concluded that scores show similarities between both models, although the HARMONIE model presents, in general, better results compared to the WRF model. Although the HARMONIE mean absolute error is slightly higher than the obtained for WRF during the pre-STC stage, the HARMONIE simulations stand out in values of mean spatial correlation, root-mean-square error, and standard deviation compared to the WRF model. In addition, during the pre-STC period, the small difference found between both models bias is also verified when comparing the WRF spatial average BT (201.43 K) with that obtained for HARMONIE (197.19 K), being the former slightly better compared to the observations (216.78 K). Evaluating the pure-STC stage, the HARMONIE mean spatial correlation, root-mean-square error, and standard deviation are above the WRF corresponding scores with the HARMONIE bias slightly worse than the obtained for WRF. In fact, despite the general underestimation found for both models compared to the observation (216.67 K), the averaged BT obtained for WRF (201.76 K) is again slightly better than the one obtained for HARMONIE (196.09 K).

Finally, it is remarkable the slight deviation of the cyclone center found by both models compared to the observations. During the pre-STC stage, the WRF model (33.67 N, −19.76 W) locates the cyclone center slightly to the north and east of the center in the images compared to the observations (33.00 N, −20.02 W). However, the HARMONIE model (33.03 N, −20.56 W) locates the cyclone center slightly to the north and west. Moreover, during the pure-STC stage, there is again a slight deviation of the cyclone center by both models. In this case, the WRF model (33.83 N, −24.01 W) locates the STC center slightly to the north and west and HARMONIE (33.42 N, −23.75 W) locates it slightly to the south and west of the observed center location (33.50 N, −23.00 W).

4. Concluding remarks

In this study, an analysis of the October 2014 STC event is assessed using two high-resolution NWP models, WRF and HARMONIE. To this end, a validation against observations is carried out. Firstly, a local analysis has been evaluated through the 2 m temperature, 2 m dew-temperature, and 10 m wind speed considering the METAR data obtained from six airports located in the Canary (GCLP and GCTS), Madeira's (LPMA and LPPS), and Azores' (LPAZ and LPPD) Islands. Moreover, the only available sounding that day located in Tenerife-Norte (GCXO) airport has also been used to evaluate the vertical behavior of both models in the STC life, taking the pre-STC and the pure-STC stages into account. Finally, an analysis of both models for the 10.8 μm IR channel from the MSG-SEVIRI satellite is evaluated. For this purpose, the BT frequency and spatial distribution and several skill scores are calculated in such stages.

The main conclusions are summarized as follows:

- Regarding the local analysis, no consistent results are in general observed between the models when analyzing the variables, i.e., 2 m temperature (Fig. 3), 2 m dew-temperature (Fig. 4), or 10 m wind speed (Fig. 5). This means that even if the WRF model is slightly better for the 2 m temperature, a similar behavior is found for both models when analyzing the 2 m dew point temperature and the 10 m wind speed, with HARMONIE performing slightly better in the Canary Islands area. Consequently, it seems to strongly depend on the area and variables analyzed per se.

- Analyzing the soundings for the temperature (Fig. 6) and wind speed (Fig. 7) through both models, it is remarkable the good results obtained in general for the WRF model, displaying less deviation compared to the HARMONIE model. Regarding the vertical temperature, it is outstanding the similar behavior of both models in the middle and higher troposphere for both analyzed dates, being the WRF model the one with slightly better results compared to HARMONIE. Besides, concerning the wind speed, a localized overestimation is obtained in low levels for the pre-STC stage for both models. Finally, during the pure-STC period, a general underestimation is obtained by both models with a slightly better behavior shown by the HARMONIE model compared to the WRF simulation. It has to be remarked that HARMONIE uses the SURFEX scheme (Masson et al., 2013), a land-ocean surface platform which has been developed by the Météo-France consortium. It is principally based on different land-surface pre-existing and well-validated models. Therefore, SURFEX gathers in its configuration all the improvements achieved in surface schemes.

- Concerning the spatial distribution, it can be noted a slight deviation to higher BTs by the HARMONIE model on the frequency distribution graph (Fig. 8), which corresponds to the simulation of fewer and lower-level clouds (Fig. 9) on both analyzed dates for the aforementioned model. However, despite this deviation, it is notable the good outcomes during the pre-STC period by this model where it is found to have similar behavior compared to the MSG-SEVIRI data, being more consistent with the observations during the pure-STC stage. Besides, it is outstanding the larger peak found at higher BTs for both models, being even more intense in the case of WRF, indicating an overestimation of the higher BT values.

- The aforementioned overestimation is also evident for both models in the spatial pattern of BT (Fig. 9). Besides, this is in agreement with the overestimation found in the 2 m dew-point temperature field (Fig. 4) for the Canary Islands' GCLP airport and Azores area, and in the sounding surface temperature results (Fig. 6). Furthermore, it is noticeable in the WRF BTs, the scattered cloudiness structure and slight absence of upper-level clouds compared to the MSG-SEVIRI data, which evidences the lack of precision of this model in the simulations of the cloudiness of the STC event. In contrast, it is noteworthy the accuracy and realism found by the HARMONIE model when simulating the clouds in comparison to the observations, highlighting the model's ability to capture the cyclone's cloud distribution.

- Moreover, regarding the skill scores results, it is remarkable the general underestimation found for both models at both analyzed dates (Table 1), which is also verified in the averaged BT for both models at the two analyzed dates, being the WRF model the one that least underestimates overall compared to the observations. Finally, regarding the location of the cyclone center during the pre-STC stage, HARMONIE tends to locate the cyclone slightly to the north and west and WRF slightly to the south and west compared to the satellite. In

Table 1
WRF and HARMONIE spatially averaged skill scores for the pre (top) and pure (bottom) STC period. The best mean spatial correlation is highlighted in bold (significant at the 0.01 level).

Pre-STC	R	BIAS	RMSE	SD	MAE
WRF	0.62	0.92	17.08	19.46	11.96
HARMONIE	0.68	0.91	17.05	21.70	12.83

Pure-STC	R	BIAS	RMSE	SD	MAE
WRF	0.57	0.93	16.94	17.75	11.86
HARMONIE	0.60	0.90	16.97	19.90	12.90

addition, both models tend to locate it slightly to the south and west compared to observations during the pure-STC period.

The obtained results and the conclusions encourage us to continue seeking the best way of analyzing this type of cyclone to improve their simulations. Additionally, the good outcomes yielded by the HARMONIE model prove that it is a useful tool, worth using in meteorological research. It has to be remarked the low computational cost of HARMONIE, because of the semi-Lagrangian advection and semi-Implicit two-time-level schemes used which generates a half time step. Moreover, the HARMONIE model configuration works with a standardized set up that provides users great versatility when the model is used. Being an NWP model of reference in several European meteorological services, more research and studies should be performed, thus persuading us to continue this line of work in the modeling of extreme events. Regarding the WRF model, future works should consider the use of other physics parameterizations, the optimization of the configuration for the grid resolutions used, as well as addressing the question of computation versus parameterization of convection in the research of STCs.

CRediT authorship contribution statement

L. Quitián-Hernández: Writing - original draft, Writing - review & editing, Methodology, Software, Visualization. **P. Bolgiani:** Software, Conceptualization, Writing - review & editing, Methodology. **D. Santos-Muñoz:** Software, Resources, Conceptualization, Writing - review & editing. **M. Sastre:** Writing - review & editing, Conceptualization, Methodology. **J. Díaz-Fernández:** Software, Methodology. **J.J. González-Alemán:** Writing - review & editing. **J.I. Farrán:** Software, Writing - review & editing. **L. Lopez:** Writing - review & editing. **F. Valero:** Supervision, Resources. **M.L. Martín:** Formal analysis, Conceptualization, Methodology, Supervision, Writing - review & editing.

Declaration of Competing Interest

The authors declare that they have no known competing financial interests or personal relationships that could have appeared to influence the work reported in this paper.

Acknowledgments

This work was partially supported by research projects: PID2019-105306RB-I00, PCIN-2014-013-C07-04, and PCIN2016-080 (UE ERA-NET Plus NEWA Project), CGL2016-78702-C2-1-R and CGL2016-78702-C2-2-R (SAFEFLIGHT project), FEI-EU-17-16 and the two ECMWF Special Projects (SPESMART and SPESVALE). JJGA is supported by the FJC2018-035821 grant and JDF acknowledges the grant supported from the MINECO-FPI program (BES-2017). The authors would like to thank Ángel García Gago for the post-processing of some figures and the skill scores calculations.

References

Arakawa, A., Wu, C.-M., 2013. A unified representation of deep moist convection in numerical modeling of the atmosphere. Part I. J. Atmos. Sci. 70, 1977–1992. https://doi.org/10.1175/JAS-D-12-0330.1.

Arakawa, A., Jung, J.-H., Wu, C.-M., 2011. Toward unification of the multiscale modeling of the atmosphere. Atmos. Chem. Phys. 11, 3731–3742. https://doi.org/10.5194/acp-11-3731-2011.

Avolio, E., et al., 2017. Sensitivity analysis of WRF model PBL schemes in simulating boundary-layer variables in southern Italy: an experimental campaign. Atmos. Res. 192, 58–71.

Aznar, R., et al., 2010. Comparison of model and satellite-derived long-term precipitation databases over the Mediterranean basin: a general overview. Atmos. Res. 97 (1–2), 170–184. https://doi.org/10.1016/j.atmosres.2010.03.026.

Bengtsson, L., et al., 2017. The HARMONIE–AROME model configuration in the ALADIN–HIRLAM NWP system. Mon. Weather Rev. 145, 1919–1935. https://doi.org/10.1175/MWR-D-16-0417.1.

Bentley, A.M., Metz, N.D., 2016. Tropical transition of an unnamed, high-latitude, tropical cyclone over the eastern North Pacific. Mon. Weather Rev. 144, 713–736. https://doi.org/10.1175/MWR-D-15-0213.1.

Bormann, N., et al., 2014. Atmospheric motion vectors from model simulations. Part I: Methods and characterization as single-level estimates of wind. J. Appl. Meteorol. Climatol. 53 (1), 47–64. https://doi.org/10.1175/JAMC-D-12-0336.1.

Chevallier, F., Kelly, G., 2002. Model clouds as seen from space: comparison with geostationary imagery in the 11-mm window channel. Mon. Weather Rev. 130, 712–722.

Davis, C.A., Bosart, L.F., 2004. The TT problem: forecasting the tropical transition of cyclones. Bull. Amer. Meteor. Soc. 85, 1657–1662.

Deng, A., Stauffer, D.R., 2006. On improving 4-km mesoscale model simulations. J. Appl. Meteorol. Climatol. 45, 361–381. https://doi.org/10.1175/JAM2341.1.

Dias Pinto, J.R., et al., 2013. Synoptic and dynamical analysis of subtropical cyclone Anita (2010) and its potential for tropical transition over the South Atlantic Ocean. J. Geophys. Res. Atmos. 118, 10870–10883. https://doi.org/10.1002/jgrd.50830.

Díaz-Fernández, J., et al., 2020. Mountain waves analysis in the vicinity of the madrid-barajas airport using the WRF model. Adv. Meteorol. 2020 https://doi.org/10.1155/2020/8871546. Article ID 8871546, 17 pages, 2020.

Dudhia, J., 1989. Numerical study of convection observed during the Winter Monsoon Experiment using a mesoscale two–dimensional model. J. Atmos. Sci. 46, 3077–3107. https://doi.org/10.1175/1520-0469(1989)046<3077:NSOCOD>2.0.CO;2.

Evans, J.L., Guishard, M.P., 2009. Atlantic subtropical storms. Part I: Diagnostic criteria and composite analysis. Mon. Weather Rev. 137, 2065–2080. https://doi.org/10.1175/2009MWR2468.1.

Fernández-González, S., et al., 2019. Forecasting of poor visibility episodes in the vicinity of Tenerife Norte Airport. Atmos. Res. 223, 49–59. https://doi.org/10.1016/J.ATMOSRES.2019.03.012.

Gerard, L., 2007. An integrated package for subgrid convection, clouds and precipitation compatible with meso-gamma scales. Q. J. R. Meteorol. Soc. 133, 711–730. https://doi.org/10.1002/qj.58.

González-Alemán, J.J., et al., 2015. Classification and synoptic analysis of subtropical cyclones within the northeastern Atlantic Ocean. J. Clim. 28, 3331–3352. https://doi.org/10.1175/JCLI-D-14-00276.1.

González-Alemán, J.J., et al., 2018. Subtropical cyclones near-term projections from an ensemble of regional climate models over the northeastern Atlantic basin. Int. J. Climatol. 38, e454–e465. https://doi.org/10.1002/joc.5383.

Grell, G.A., Freitas, S., 2013. A scale and aerosol aware stochastic convective parameterization for weather and air quality modeling. Atmos. Chem. Phys. Discuss. 13 https://doi.org/10.5194/acpd-13-23845-2013, 23 845-23 893.

Grell, E., Grell, G., Bao, J.-W., 2013. Experimenting with a convective parameterization scheme suitable for high resolution mesoscale models in tropical cyclone simulations. Geophys. Res. Abstr. 15. EGU2013–5746-2. [Available online at http://meetingorganizer.copernicus.org/EGU2013/EGU2013-5746-2.pdf.].

Guishard, M.P., et al., 2007. Bermuda subtropical storms. Meteorog. Atmos. Phys. 97, 239–253. https://doi.org/10.1007/s00703-006-0255-y.

Hariprasad, K.B.R.R., et al., 2014. Numerical simulation and intercomparison of boundary layer structure with different PBL schemes in WRF using experimental observations at a tropical site. Atmos. Res. 145, 27–44.

Hart, R.E., 2003. A cyclone phase space derived from thermal wind and thermal asymmetry. Mon. Weather Rev. 131, 585–616. https://doi.org/10.1175/1520-0493(2003)131,0585:ACPSDF.2.0.CO;2.

Hayashi, S., et al., 2008. Statistical verification of short-term NWP by NHM and WRF-ARW with 20 km horizontal resolution around Japan and Southeast Asia. Sola 4, 133–136.

Hazra, V., Pattnaik, S., 2020. Systematic errors in the WRF model planetary boundary layer schemes for two contrasting monsoon seasons over the state of Odisha and its neighborhood region. Theor. Appl. Climatol. 139 (3), 1079–1096.

Hohenegger, C., Schär, C., 2007. Predictability and Error Growth Dynamics in Cloud-Resolving Models. J. Atmos. Sci. 64 (12), 4467–4478.

Hong, S.-Y., Lim, J.-O.J., 2006. The WRF single-moment 6–class microphysics scheme (WSM6). J. Korean Meteor. Soc. 42, 129–151.

Hu, X.M., et al., 2010. Evaluation of three planetary boundary layer schemes in the WRF model. J. Appl. Meteorol. 49, 1831–1844.

Jankov, I., et al., 2011. An evaluation of five WRF-ARW microphysics schemes using synthetic GOES imagery for an atmospheric river event affecting the California coast. J. Hydrometeorol. 12, 618–633. https://doi.org/10.1175/2010JHM1282.1.

Kanase, R.D., Salvekar, P.S., 2014. Study of weak intensity cyclones over Bay of Bengal using WRF model. Atmos. Climate Sci. 4, 534–548.

Kanase, R.D., Salvekar, P.S., 2015. Effect of physical parameterization schemes on track and intensity of cyclone LAILA using WRF model. Asia-Pacific. J. Atmos. Sci. 51 (3), 205–227.

Kotroni, V., Lagouvardos, K., 2004. Evaluation of MM5 high resolution real-time forecasts over the urban area of Athens, Greece. J. Appl. Meteorol. 43, 1,666–1,678. https://doi.org/10.1175/JAM2170.1.

Lamraoui, F., et al., 2018. The interaction between Boundary Layer and Convection Schemes in a WRF simulation of Post Cold Frontal Clouds over the ARM East North Atlantic site. J. Geophys. Res. Atmos. 124, 4699–4721. https://doi.org/10.1029/2018JD029370.

Liu, Y.B., Zhang, D.L., Yau, M.K., 1997. A multiscale numerical study of Hurricane Andrew (1992). Part I: Explicit simulation and verification. Mon. Weather Rev. 125, 3,073–3,093, doi:10.1175/1520-0493(1997)125<3073: AMNSOH>2.0.CO;2.

Loew, A., et al., 2017. Validation practices for satellite-based Earth observation data across communities. Rev. Geophys. 55 (3), 779–817.

López, L., et al., 2007. A short-term forecast model for hail. Atmos. Res. 83 (2–4), 176–184. https://doi.org/10.1016/j.atmosres.2005.10.014.
Masson, et al., 2013. The SURFEXv7.2 land and ocean surface platform for coupled or offline simulation of earth surface variables and fluxes. Geosci. Model Dev. 6, 929–960. https://doi.org/10.5194/gmd-6-929-2013.
Montejo, I.B., 2016. Sensitivity study of the cloudiness forecast of the WRF model in the western half of Cuba. Revista Cubana de Meteorología 22 (1), 66–80. https://doi.org/10.1155/2018/1381092.
Neyestani, A., et al., 2018. Inter-comparison of HARMONIE and WRF model simulations in convective-permitting scale over western area of Iran. Iran. J. Geophys. 12 (1), 1–18.
Otkin, J.A., Greenwald, T.J., 2008. Comparison of WRF model-simulated and MODIS-derived cloud data. Mon. Weather Rev. 136, 1957–1970.
Otkin, J.A., Greenwald, T.J., Sieglaff, J., Huang, H.L., 2009. Validation of a large-scale simulated brightness temperature dataset using SEVIRI satellite observations. J. Appl. Meteorol. Climatol. 48 (8), 1613–1626. https://doi.org/10.1175/2009JAMC2142.1.
Pasternak, F., et al., 1994. Spinning enhanced visible and infrared imager (SEVIRI): the new imager for Meteosat second generation. In: Space Optics 1994: Earth Observation and Astronomy, 2209. International Society for Optics and Photonics, pp. 86–94. https://doi.org/10.1117/12.185247.
Quitián-Hernández, et al., 2016. Identification of a subtropical cyclone in the proximity of the Canary Islands and its analysis by numerical modeling. Atmos. Res. 178-179, 125–137. https://doi.org/10.1016/j.atmosres.2016.03.008.
Quitián-Hernández, et al., 2018. Analysis of sensitivity to different parameterization schemes for a subtropical cyclone. Atmos. Res. 204, 21–36. https://doi.org/10.1016/j.atmosres.2018.01.001.
Quitián-Hernández, et al., 2020. Subtropical cyclone formation via warm seclusion development: the importance of surface fluxes. J. Geophys. Res. Atmos. 125 (8) https://doi.org/10.1029/2019JD031526 (2020), e2019JD031526.
Román-Cascón, C., et al., 2019. Radiation and cloud-base lowering fog events: observational analysis and evaluation of WRF and HARMONIE. Atmos. Res. 229, 190–207.
Santos-Muñoz, D., 2015. HIRLAM Consortium. Validation of HARMONIE-40h1. Consulted in 2020. Retrieve from. https://hirlam.org/portal/validation/40h1/AIC-feb2010/index.html.
Shapiro, M.A., Keyser, D., 1990. Fronts, jets streams, and the tropopause. In: Newton, C. W., Holopainen, E. (Eds.), Extratropical Cyclones: The Erik Palmén Memorial Volume. American Meteorological Society, pp. 167–191.
Shi, X., et al., 2018. Simulation of FY-2D infrared brightness temperature and sensitivity analysis to the errors of WRF simulated cloud variables. Sci. China Earth Sci. 61, 957–972. https://doi.org/10.1007/s11430-017-9150-0.
Shimada, S., et al., 2011. Accuracy of the wind speed profile in the lower PBL as simulated by the WRF model. Sola 7, 109–112. https://doi.org/10.2151/sola.2011-028.
Skamarock, W.C., Klemp, J.B., 2008. A time-split non-hydrostatic atmospheric model for weather research and forecasting applications. J. Comput. Phys. 227 (7), 3465–3485. https://doi.org/10.1016/j.jcp.2007.01.037.
Steward, S.R., 2001. Tropical Cyclone Report: Hurricane Karen, 12–15 October 2001. National Hurricane Center (10 pp.).
Sun, Y., Lan, Y., Zhong, Z., Hu, Y., Ha, Y., 2013. Dependence of model convergence on horizontal resolution and convective parameterization in simulations of a tropical cyclone at gray-zone resolutions. J. Geophys. Res. - Atmos. 118, 7715–7732.
Sun, Y., Yi, L., Zhong, Z., Ha, Y., 2014. Performance of a new convective parameterization scheme on model convergence in simulations of a tropical cyclone at grey-zone resolutions. J. Atmos. Sci. 71, 2078–2088.
Tiedtke, M., 1989. A comprehensive mass flux scheme for cumulus parameterization in large-scale models. Mon. Weather Rev. 117, 1779–1800.
Toros, H., et al., 2018. Simulating heavy precipitation with HARMONIE, HIRLAM, and WRF-ARW: a flash flood case study in Istanbul, Turkey. Eur. J. Sci. Technol. 13, 1–12.
Uboldi, F., Trevisan, A., 2015. Multiple-scale error growth in a convection-resolving model. Nonlin. Processes Geophys. 22, 1–13. https://doi.org/10.5194/npg-22-1-2015.
Weisman, M.L., et al., 2008. Experiences with 0–36-h Explicit Convective forecasts with the WRF-ARW Model. Weather Forecast. 23 (3), 407–437.
WWRP (World Weather Research programme), WGNE (Working Group on Numerical Experimentation) Joint Working Group on Forecast Verification Research, 2017. Forecast Verification Methods across Time and Space Scales. 7th International Verification Methods Workshop. Available at. https://www.cawcr.gov.au/projects/verification/#Standard_verification_methods.
Yang, X., 2008. Development of HIRLAM/HARMONIE monitoring system. HIRLAM Newslett. 54.
Zhang, F., et al., 2007. Mesoscale Predictability of Moist Baroclinic Waves: Convection-Permitting experiments and Multistage Error Growth Dynamics. J. Atmos. Sci. 64 (10), 3579–3594.
Zingerle, C., 2005. Satellite Data in the Verification of Model Cloud forecasts: a convective case in summer 2003 seen from NOAA satellites. Hirlam Newslet. 48, 173–177.